Available online at www.sciencedirect.com
ScienceDirect
Ceramics International 35 (2009) 349–358
CERAMICS INTERNATIONAL
www.elsevier.com/locate/ceramint

Preparation and properties of C/SiC/ZrO_2 porous composites by hot isostatic pressing the pyrolyzed preforms

Muhammad Akhtar Sharif, Hidekazu Sueyoshi *

Department of Nano-structure and Advanced Materials, Graduate School of Science and Engineering, Kagoshima University, Korimoto 1-21-40, Kagoshima Shi 890-0065, Japan

Received 5 September 2007; received in revised form 29 September 2007; accepted 4 November 2007
Available online 1 February 2008

Abstract

Three phase mixture of C/SiC/ZrO_2 porous composites were prepared from commercially available phenolic resin, Si and ZrO_2 powders. In the first step, mixed powders were pyrolyzed at 850 °C in vacuum to obtain a carbonized microporous material and then hot isostatically pressed at 1200, 1300 and 1350 °C for 10 min in an argon pressure of 50 MPa to prepare C/SiC/ZrO_2 porous composites, in second step. The hot isostatic pressing led to the increase in density from 3.28 to 3.48 g/cm^3 and reduction in porosity (from 32 to 20%) of the composites. X-ray diffraction analyses revealed the existence of β-SiC and carbon might be amorphous in the composites. According to the results of scanning electron microscopy, the crystal growth of β-SiC with facets was observed at 1350 °C. In addition, the energy dispersive spectroscopy showed that carbon/silicon atomic ratio was 1:1 in the crystals. X-ray photoelectron spectroscopy of the composites suggested that evolved gaseous molecules, due to the decomposition of phenolic resin, reacted with molecules containing Si to form β-SiC. The formation and growth of β-SiC in addition to the densification of matrix by hot isostatic pressing led to the increase in hardness (max.: 13.99 GPa) at higher temperatures.
© 2007 Elsevier Ltd and Techna Group S.r.l. All rights reserved.

Keywords: A. Hot isostatic pressing; B. Composites; E. Functional applications; β-SiC

1. Introduction

Recently, the interest of porous ceramic composites has significantly increased due to their applications, e.g., environmental filters, gas/liquid separators, light weight structural materials, biomaterials, thermal insulators, sensors, etc. [1–10]. However, the strength of porous ceramics is considerably low as compared to dense ceramics. Therefore, it is necessary to improve the strength and toughness of porous ceramics in order to widen their applications. One of the strengthening methods of the porous ceramics is to use composite routes using particles, whiskers, or platelets at reinforcements [11,12]. In addition, the introduction of small pores into the matrix is favored because fracture strength of brittle materials decreases with increasing flaw size. In order to attain these strengthening effects simultaneously during the synthesis of porous ceramics, it is necessary to prepare preforms of ceramic–matrix-composites (CMCs) in which fine pores and second particles are uniformly distributed.

Ceramic matrix composites reinforced with SiC particles, whiskers, or platelets have received increasing attention due to their potentially high fracture toughness and strength [13,14] because silicon carbide has high melting point, high hardness, high abrasion resistance, good chemical resistance, good radiation resistance, good thermal conductivity, low thermal expansion coefficient and high thermal shock resistance. In ceramic composites reinforced with SiC particles, in situ formation of SiC provides an effective way for uniform dispersion of SiC in the matrix. Good mixing is attainable between ceramic powders and SiC precursors (rather than fine SiC particles) because the SiC precursors are usually silicon-containing polymers or gels [15]. Precursors may also be formed by making slurry of polymer and silicon powders. After suitable heat treatments, the precursors convert into fine SiC particles with uniform dispersion. As for densification of ceramic/SiC composites, limited progress has been achieved so far. Whether the SiC particles are physically mixed or in situ reaction-formed, most of the ceramic/SiC

* Corresponding author. Tel.: +81 99 285 7704; fax: +81 99 285 7704.
E-mail address: sueyoshi@mech.kagoshima-u.ac.jp (H. Sueyoshi).

0272-8842/$34.00 © 2007 Elsevier Ltd and Techna Group S.r.l. All rights reserved.
doi:10.1016/j.ceramint.2007.11.002

composites are densified by pressure-assisted sintering (hot isostatic pressing).

Phenolic resins, including thermosetting ones, are widely used as coatings, adhesives, composites, etc., due to their excellent flame resistance, heat resistance, insulativity, dimensional stability and chemical resistance. However, great care has been taken to the disposal of used phenolic resin products because their superior properties make them very difficult to degrade and recycle. During the pyrolysis of phenolic resin, weight loss occurs at about 200 °C and rapidly develops above 450 °C, indicating the formation of a great deal of gases (such as CH_4, H_2, CO, CO_2, H_2O, etc.) [16]. In addition, the development of cabonized porous structure starts above 450 °C and in the range 800–900 °C results microporous materials with relatively high sorption capacity and molecular sieve properties. The incorporation of polymer, like phenolic resin, into the fabrication of porous ceramic composites coupled with the pyrolysis route is expected to provide one of the recycling methods for used polymeric products.

The aim of the present study is to prepare C/SiC/ZrO_2 porous composites from commercially available phenolic resin/Si/ZrO_2 powders by in situ formation of β-SiC and densification by hot isostatic pressing. In the first step, mixed powders were pyrolyzed at 850 °C in vacuum to obtain a carbonized microporous material and then hot isostatically pressed at 1200, 1300 and 1350 °C for 10 min in an argon pressure of 50 MPa to prepare densified C/SiC/ZrO_2 porous composites, in second step.

2. Experimental procedure

2.1. Materials

Powders of a novolac-type phenol resin (PR-50590B, Sumitomo Bakelite Co. Ltd., Japan), Si (Furuuchi Chemical Co. Ltd., Japan) and ZrO_2 (TOSOH-ZIRCONIA TZ-0, TOSOH Co. Ltd., Japan) were used as starting materials. The average grain sizes of the phenol resin, Si and ZrO_2 powders were 35, 1 and 0.40 μm, respectively. The mass ratio of the phenol resin, Si and ZrO_2 powders was 2:1:1, respectively.

2.2. Sample preparation

Si and ZrO_2 powders were mixed in a grinding bowl for 3 h. Phenol resin of 50 g was dissolved in 28 ml of ethanol at room temperature and then added to the mixture of Si/ZrO_2 powders to make slurry. The slurry was poured into copper tubes with an inner diameter of 8 mm and 1 mm in thickness. The partial sealing of slurry was conducted by mechanical pressing the both ends of copper tubes, which prevented the failure or ballooning of the tubes due to the increase in internal pressure with temperature.

The pyrolysis of the mixture (slurry) was carried out by heating the copper tubes in vacuum (0.015 Pa). Since the pyrolysis of phenolic resin starts at about 200 °C, therefore, copper tubes (containing slurry) were heated from room temperature to 200 °C at a slow heating rate (200 °C/h) to avoid the formation of large pores due to the evolution of large amount of gases at higher heating rate, kept at this temperature for 1 h and then heated to 850 °C in 3 h to obtain a carbonized microporous materials (here called as pyrolyzed composites/preforms), kept at this temperature for 3 h. Cooling was also done in two steps. In the first step, copper tubes were cooled down at 450 °C with a slow cooling rate (200 °C/h) so that the preforms could shrink very well that might help while removing from the copper tubes and then at room temperature. The pyrolyzed phenol resin/Si/ZrO_2 composites with a diameter comparable to the inner diameter of the copper tubes were obtained.

After the pyrolysis, the preforms were wrapped with zirconia fabric (to avoid the sticking of preforms on the inner surfaces of steel case) and then enclosed in steel cases (0.6 mm thick: SPCEN-NUD, Nisshin Steel Co. Ltd., Japan). The edges of the steel cases were welded to suppress the emission of gases from the composites completely. In order to prepare C/SiC/ZrO_2 porous composites, the steel cases containing preforms were hot isostaically pressed (HIPed) at 1200, 1300 and 1350 °C (below the melting point of Si) for 10 min in an argon atmosphere of 50 MPa. As hot isostatic pressing is a faster process, therefore heating and cooling rates during HIPing process were 600 °C/h. The composites HIPed at 1200, 1300 and 1350 °C were named as ZRS12, ZRS13 and ZRS135, respectively.

2.3. Properties and microstructural investigations

The densities of the composites were measured by Archimedes method and open porosities were measured by boiling water penetration method (specimens were put in boiling water for 2 h and then kept in water for 18 h). Vickers microhardness of matrices was measured by using Vickers microhardness tester (HMV, Shimadzu Co. Ltd., Japan). A load of 9.807 N was applied for 30 s. Microstructures of the polished specimens were observed by using scanning electron microscopy (SEM: XL-30 ESEM, FEI Company Ltd., Japan). Elemental analysis was also carried out at several points of the observed area by using EDS (energy dispersive spectroscopy) equipped to the SEM. The structures of crystals involved in the composites were identified with the X-ray diffraction (XRD: RIGAKU, Geigerflex 2013), which was performed with Cu Kα irradiation (0.15406 nm) at a scanning rate of 2°/min in 2θ range between 20° and 80°. Chemical states of atoms in the composites were investigated by X-ray photoelectron spectroscopy (XPS: ESCA-1000, Shimadzu Co. Ltd., Japan) with Mg Kα irradiation (1.253 keV). Since the specimens were exposed to air, their surfaces were removed by argon ion (Ar^+) milling for 5 min before the XPS analyses.

3. Results

3.1. Apparent density and open porosity

Fig. 1 shows the effect of temperature on the apparent density and open porosity of the HIPed composites. The

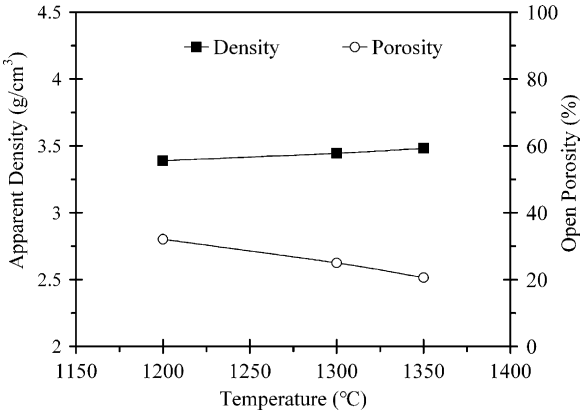

Fig. 1. Effect of temperature on the apparent density and open porosity of the HIPed composites.

increase in density and decrease in porosity of the composites was observed when HIPed at higher temperatures. But, when the interlinked pores or open pores in the composites become isolated upon densification then the gases trapped in the pores act against the pressure applied for pore reduction (i.e. argon pressure) and resulted in the decrease in densification rate at higher temperatures. The results showed that HIPing led to the increase in density from 3.38 to 3.48 g/cm^3 and reduction in porosity (from 32 to 20%) of the composites.

3.2. Vickers microhardness

Vickers microhardness of the composites was increased with HIPing temperature, as shown in Fig. 2. In addition to the densification by HIPing process, the formation and growth of β-SiC particles (will be discussed in coming sections) at higher temperatures caused the increase in volume fraction of β-SiC particles associated with the decrease in the volume fraction of matrix. Therefore, the formation and growth of β-SiC in addition to the densification of matrix by HIPing led to the rapid increase in hardness of the composites. The maximum Vickers microhardness (13.99 GPa) was obtained from ZRS135, which is more than the bulk hardness of zirconia (10–12 GPa).

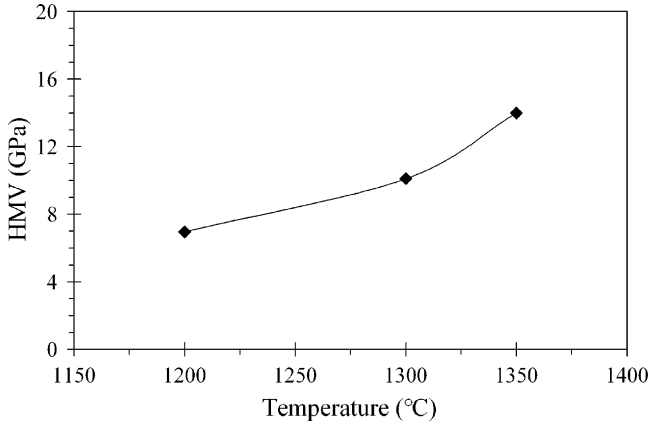

Fig. 2. Change in Vickers microhardness of the composites HIPed at various temperatures.

3.3. X-ray diffraction (XRD)

Fig. 3 shows the XRD spectra obtained from ZRS12, ZRS13 and ZRS135 composites. The peaks at $2\theta = 28.4^\circ$, 47.3°, 56.1° belong to (1 1 1), (2 2 0) and (3 1 1) planes of cubic crystalline silicon [17]. ZrO_2 has monoclinic form with peaks (−1 1 1), (1 1 1), (2 0 0) and (0 0 2) at $2\theta = 28.1^\circ$, 31.4°, 34.1° and 35.3°, respectively [2]. Since monoclinic ZrO_2 changes to tetragonal ZrO_2 at 1170 °C [18,19], this fact is also shown by the HIPed composites. Other peaks of Si and ZrO_2 are also indexed in Fig. 3. X-ray diffraction peaks around $2\theta = 35.6^\circ$, 41.4°, 60.0° and 71.8° are (1 1 1), (2 0 0), (2 2 0) and (3 1 1) belong to cubic form silicon carbide (β-SiC), respectively [20,21]. The peaks of carbon were not observed in XRD profile, which means that amorphous carbon exists in the pyrolyzed specimens. The peak height of β-SiC increases with the HIPing temperature, while that of Si decreases (Fig. 3). Most of the Si powders converted to β-SiC when the composite was HIPed at 1350 °C. This result also shows that most of the C atoms formed due to the decomposition of phenolic resin were consumed in the formation and growth of β-SiC.

3.4. Microstructure

Fig. 4 shows SEM micrographs of cross-sections of the polished specimens. The composite ZRS12 (Fig. 4) exhibits numerous pores with diameters ranging from several μm to several 10 μm. The evolution of volatile products (such as CH_4, H_2, CO, CO_2, H_2O, etc.) due to thermal decomposition of phenolic resin caused the formation of these pores. A certain fraction of the pores were filled with particles (Fig. 4), which resulted in the increase in density of the composites. The white regions indicate that some reactions took place during HIPing process, and the increase in area of these places suggested that rate of reaction was increased at higher temperatures, as shown in Fig. 4. This result is in agreement with XRD results, where the formation of β-SiC was enhanced at higher HIPing temperatures.

Fig. 5 shows the enlarged SEM images of the particles in pores of the composites. The filling of pores with particles (D, E, F, etc.) can be well understood from Fig. 5. The particles (e.g. particle D in Fig. 5(a)) have irregular shapes in the composite

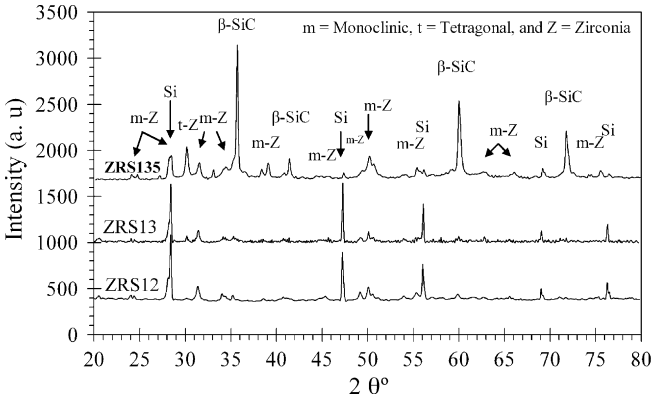

Fig. 3. X-ray diffraction spectra obtained from the composites.

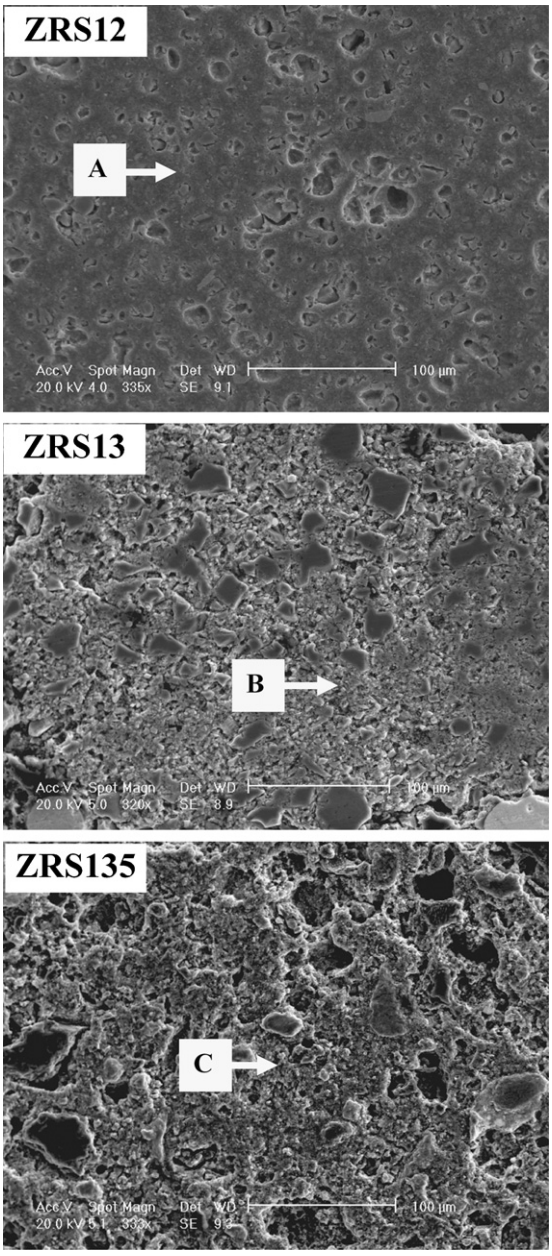

Fig. 4. SEM micrographs of cross-sections of the polished specimens.

ZRS12. According to the XRD result, the amount of β-SiC formed at this temperature is considered to be small to make an effect on the morphology of the composites. The particles (e.g. particle E in Fig. 5(b)) gained some regularity in the composite ZRS13, while the particles (e.g. particle F in Fig. 5(c)) in the composite ZRS135 have regularity in their shapes and are partly truncated with facets, which is characteristic of β-SiC particles. Fig. 5(d) shows the enlarged view of the encircled pore particle (F in Fig. 5(c)) with regular facets in the composite ZRS135, where β-SiC dominates in the XRD spectrum, the most of the Si powders converted to β-SiC particles with polyhedral shapes. The polyhedral β-SiC has symmetrical surfaces of the equilateral triangle, rectangle, trapezoid, hexagon and so on.

In one of our special experiment, when the ZRS85 was HIPed at 1400 °C (below the melting point of Si), SEM observations revealed the formation of crystals and long whiskers with diameters less than 100 nm, as shown in Fig. 5(e and f). Since the atomic fractions of the elements in the crystals and whiskers were found to be nearly 50% Si and 50% C by means of the EDS analyses and no peaks of α-SiC appeared in the XRD spectrum, therefore, these crystals and whiskers were assigned to be β-SiC. However, the growth of long SiC whiskers might be due the reaction of gaseous molecules containing Si and C atoms.

3.5. Elemental analyses (EDS)

Fig. 6 shows the EDS spectra obtained from the matrices of the ZRS12, ZRS13 and ZRS135 composites, corresponding to region A, B and C in Fig. 4, respectively. It is obvious that Si has the highest peak (as compared to the peaks of Zr, C and O) in the matrices of all composites, according to the EDS spectra. The peak height and area of C peak decreases with increasing temperature, while those of Si peak remain nearly constant. The peak height and area of Zr peak decreases up to 1300 °C, and then, remain nearly constant up to1350 °C. EDS analyses also showed the low peaks of O in all the matrices of HIPed composites. Since the characteristic X-rays are emitted from the region with a radius of several μm under the surface, the spectra of Fig. 6 imply the content of C, Zr, O and Si atoms in this region. Hence the Si peak with nearly the same area or height indicates that the volume of Si particles in the region of characteristic X-ray emission is nearly constant irrespective of temperature. On the other hand, the decrease of C content from 1200 to 1350 °C indicates that the thermal decomposition of the matrix of the pyrolyzed composite continues to take place at the HIP temperatures, and C atoms (formed due to carbonization of phenolic resin) or C containing molecules (e.g. CH_4, CO, CO_2, etc.) are removed from the matrix. Therefore, C atoms or C containing molecules might be reacted with the Si containing molecules to form β-SiC particles.

The EDS analyses conducted on the surfaces of pore particles (D, E and F in Fig. 5) showed small C peak in comparison to that of matrix at each temperature, while that of Si remained constant as that in case of matrices, as shown in Fig. 7. EDS analyses showed the low peaks of Zr and O atoms involved in the pore particles (D and E) of the ZRS12 and ZRS13 composites. These might be due to the embedded nano-ZrO_2 particles in the pore particles. On the other hand, peaks of Zr and O were not observed in the pore particle (F) of the ZRS135 composite. This means that zirconia is not involved in pore particles in the composite HIPed at 1350 °C. In addition, the EDS analyses showed that C/Si atomic ratio is nearly 1:1 in the pore particle of ZRS135 composite. This C/Si atomic ratio may be reasonable to be assigned to that of β-SiC, because XRD analysis of ZRS135 composite also showed the prominent appearance of β-SiC.

3.6. XPS investigations

X-ray photoelectron spectroscopy (XPS) is a unique and unparalleled instrumental technique for obtaining detailed

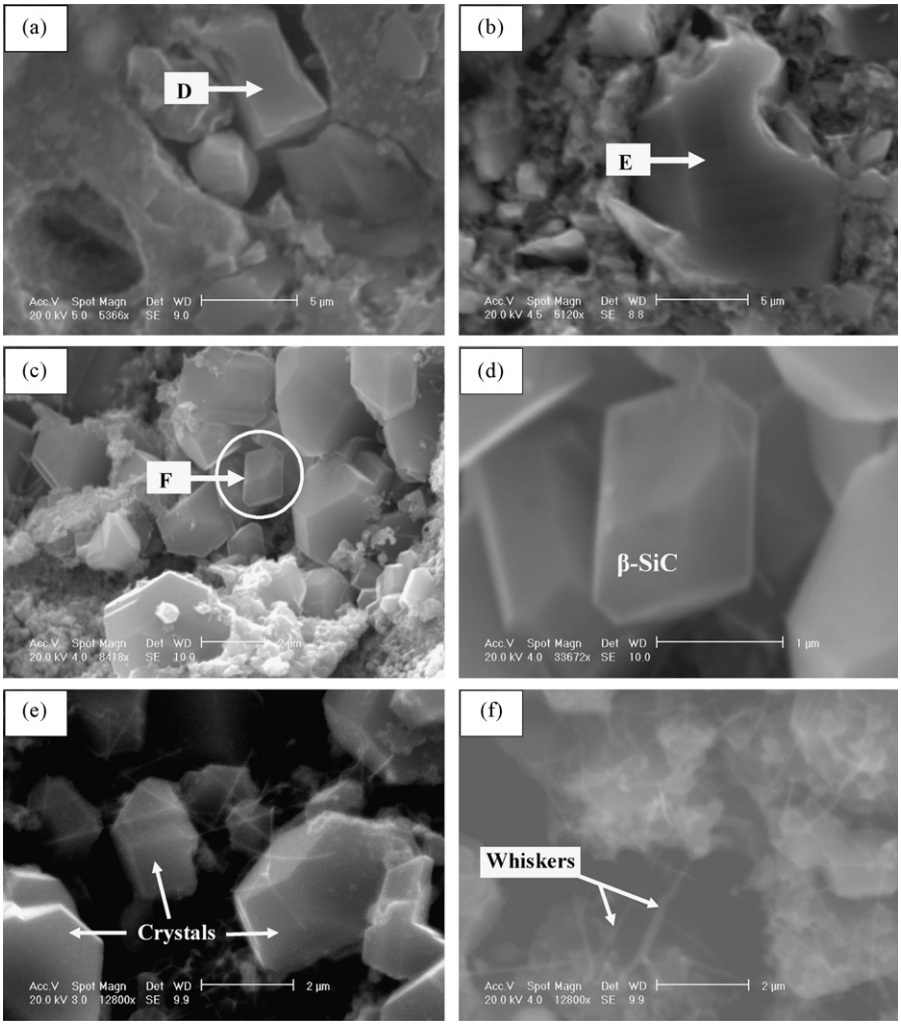

Fig. 5. Enlarged SEM images of the particles in pores of the composites (a) ZRS12, (b) ZRS13, (c) ZRS135 and (d) Pore particle (F: in Fig. 5(c)) and (e, f) crystals and whiskers formed in the composite HIPed at 1400 °C.

atomic elemental information and only non-destructive spectroscopic technique that can also yield data on molecular structures [22]. Thus, the observed XPS spectra of Si, C, Zr and O are mentioned below.

3.6.1. Silicon

XPS spectra of Si $2p^{3/2}$ electrons obtained from the ZRS12, ZRS13 and ZRS135 composites are shown in Fig. 8. The peak at lower energy arises from Si $2p^{3/2}$ (99.60 eV) of metallic Si (Si^0). The spectrum is broadened towards higher energies indicates that Si atoms are bound with other atoms. The peak at 101.00 eV corresponds to SiC, whose existence in cubic form was also observed in XRD analyses. The peak height of SiC increases with temperature and becomes highest in XPS spectrum obtained from the ZRS135 composite and this agrees with the results of XRD analyses where the peak height of SiC is heightened. It is reasonable to consider that XPS spectrum for Si $2p^{3/2}$ has a range where chemical state of Si varies continuously from mono-oxide to fully oxidized state of dioxide. Remarkable peaks are attributed to oxide layers of Si such as SiO and SiO_2. The peak at 102.30 eV corresponds to the deposited thin layer (about 300 nm) of SiO [23], and peak at the highest binding energy of 103.60–103.80 eV belongs to SiO_2. The peak height of SiO_2 decreases (Fig. 8) with the rise in HIPing temperature, which indicates the reduction of oxidized Si powders. On the other hand, the increase in peak height of SiO might be due the reduction of SiO_2 to SiO or it might be due the formation of SiO by the reaction of Si and gases formed during pyrolysis. The formed SiO and SiO_2 may be amorphous because XRD pattern of the composites did not reveal their crystalline existence.

3.6.2. Carbon

Fig. 9 shows the XPS spectra of C 1s electrons obtained from the HIPed composites. The XPS spectra are broadened towards high-energy side and have several peaks. The highest peak at 284.40 eV originated from carbon (C–C) or hydrocarbons (C–H) present in the HIPed composites. The peak height of carbon almost remained same in the ZRS12 and ZRS13 composites, while the peak height of carbon is decreased in the ZRS135 composite. This decrease in peak height of carbon might be due to its consumption for the formation of compounds containing

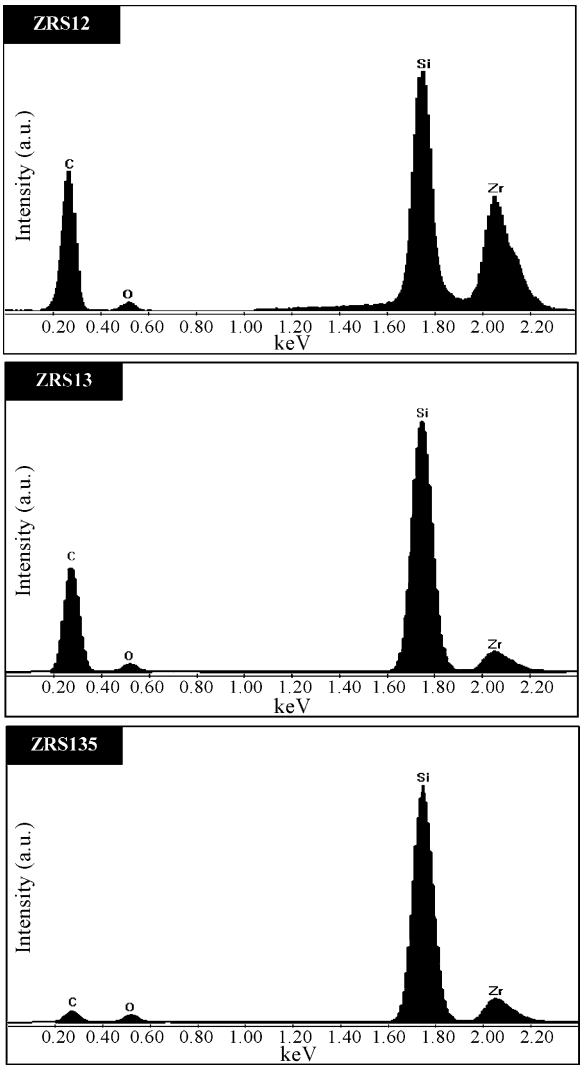

Fig. 6. EDS analyses of the matrices (points A, B and C in Fig. 4) of the composites.

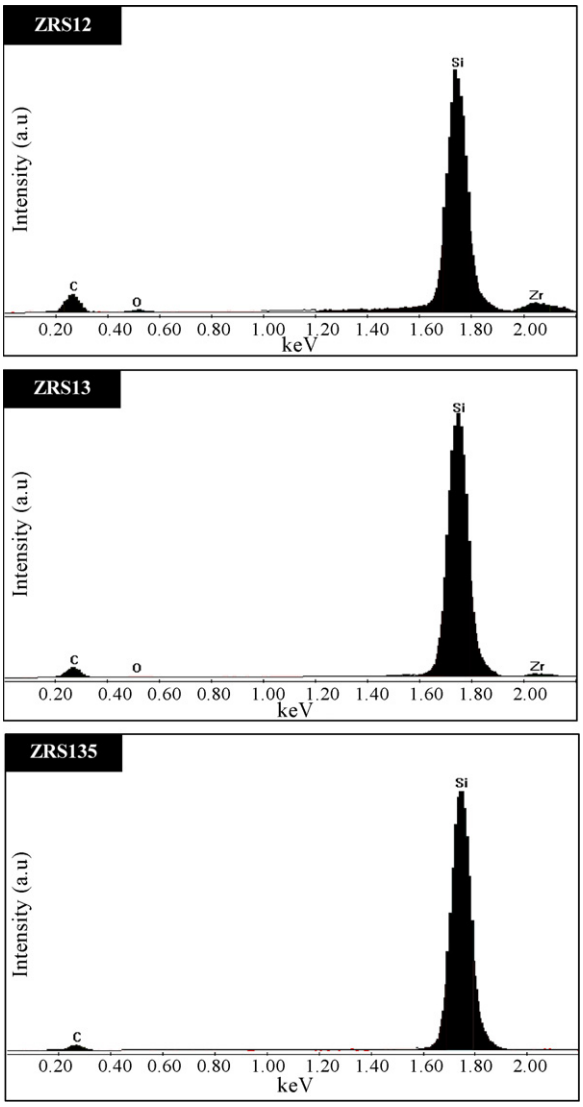

Fig. 7. EDS spectra obtained from the particles in pores (D, E and F in Fig. 5) of the composites.

carbon like SiC, CO and CO_2, etc. The other peaks are divided into lower and higher ones than 284.40 eV. The lower energy peak around 283.00 eV is considered to be attributed to C 1s in SiC. The formation of SiC was also observed in XRD analyses of the composites and XPS spectra for Si 2p electrons. The XPS spectrum obtained from ZRS135 composite showed that the peak height of SiC is higher than those in ZRS12 and ZRS13 composites. This result is in agreement with the XRD analyses and XPS spectra for Si 2p electrons. The other higher energy peak around 285.75 eV is assigned to hydroxyl (>C–OH) and around 287.75 eV is assigned to carbonyl functional group (>C=O). These results suggest that formation of various organic compounds with different functional groups took place during HIPing process that caused the porous structure of the composites.

3.6.3. Zirconium

XPS spectra of Zr 3d electrons obtained from ZRS12, ZRS13 and ZRS135 composites showed almost the similar behavior as shown in Fig. 10. Zirconium is involved in ZrO_2 for its $3d^{5/2}$ and $3d^{3/2}$ electrons at 182.40 and 184.85 eV, respectively. The decomposition of ZrO_2 into other compounds like ZrC or $ZrSiO_4$ could not be observed from XPS spectra (Fig. 10).

3.6.4. Oxygen

The XPS spectra of O 1s electrons obtained from HIPed composites are shown in Fig. 11. The XPS spectra revealed the presence of four peaks corresponding to ZrO_2 (around 530 eV), carbonyl (>C=O) or hydroxyl (>C–OH) group at 531.70 eV, SiO (around 532.40 eV) and SiO_2 between 533.40 and 533.90 eV, respectively. The peak height of SiO_2 decreases with HIPing temperature might be indicating the reduction of SiO_2, while the peak height of SiO is heightened with temperature representing the existence of more formed deposited vapors of SiO. XPS spectra for Zr 3d and Si 2p electrons also showed the existence of oxygen involved in ZrO_2, SiO_2 and SiO. The formation of organic compounds

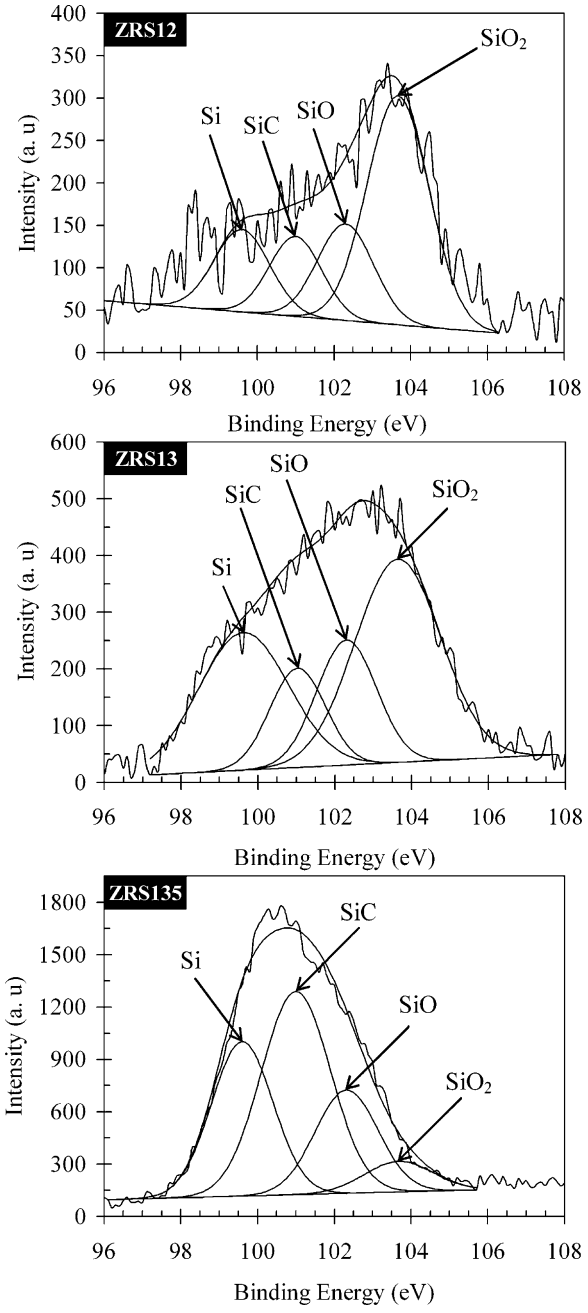

Fig. 8. XPS spectra of Si $2p^{3/2}$ electrons.

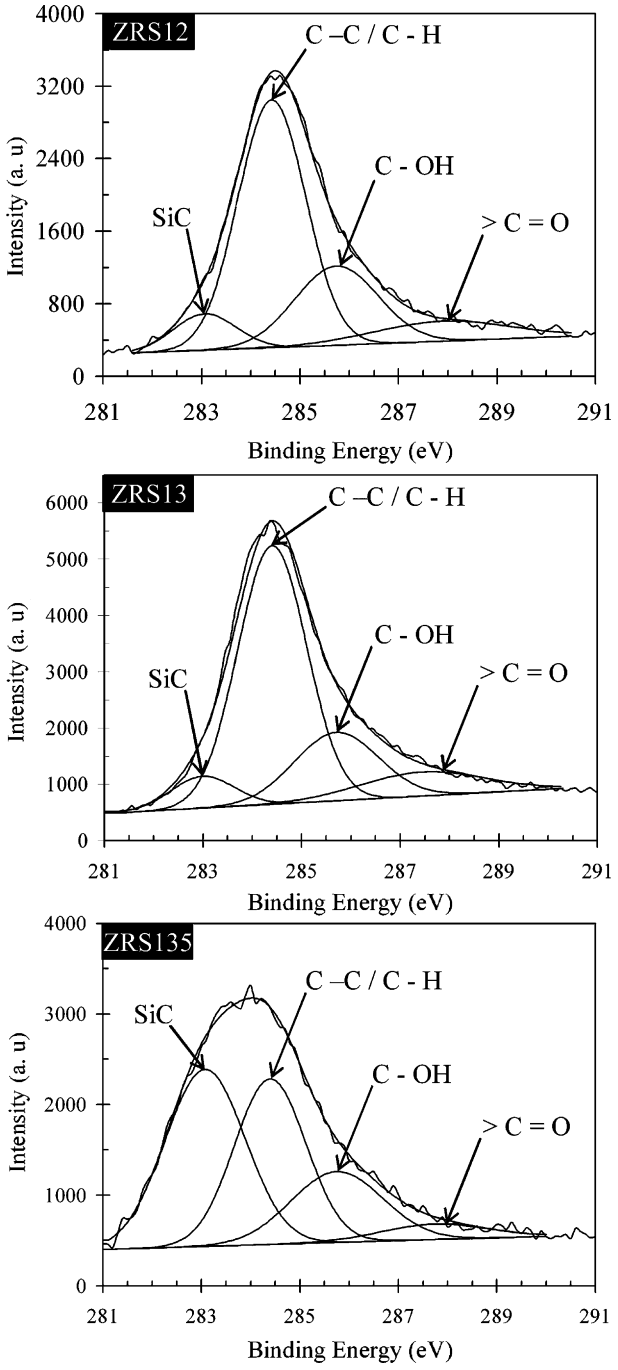

Fig. 9. XPS spectra of C 1s electrons.

containing carbonyl and alkyl hydroxyl groups was also revealed by XPS spectra of C 1s electrons. These gaseous compounds were produced during pyrolysis of phenol resin and caused the formation of pores. Those gaseous compounds, which trapped in closed pores were deposited on the inner surfaces of pores.

4. Discussion

The pyrolysis of phenolic resin is accompanied with the evolution of gases e.g. H_2, CO_2, CH_4, H_2O, C, CO, etc. [16,24]. Fig. 12 shows relationship between the change in Gibbs free energy and temperature for the formation of various compounds. The change in Gibbs free energies of CO and SiO are very closely related to each other (Fig. 12). The evolution of gaseous species during pyrolyses is might be necessary for the formation of whisker β-SiC. In addition to the degasification during pyrolyses, the pyrolysis reactions convert phenolic matrix to amorphous carbon [16], the absence of carbon peaks in the XRD analyses (Fig. 3) verified this result. XPS analyses also suggested the formation SiO, SiO_2 and SiC. According to SEM analyses, the evolution gaseous products during pyrolysis caused the formation of voids in the composites.

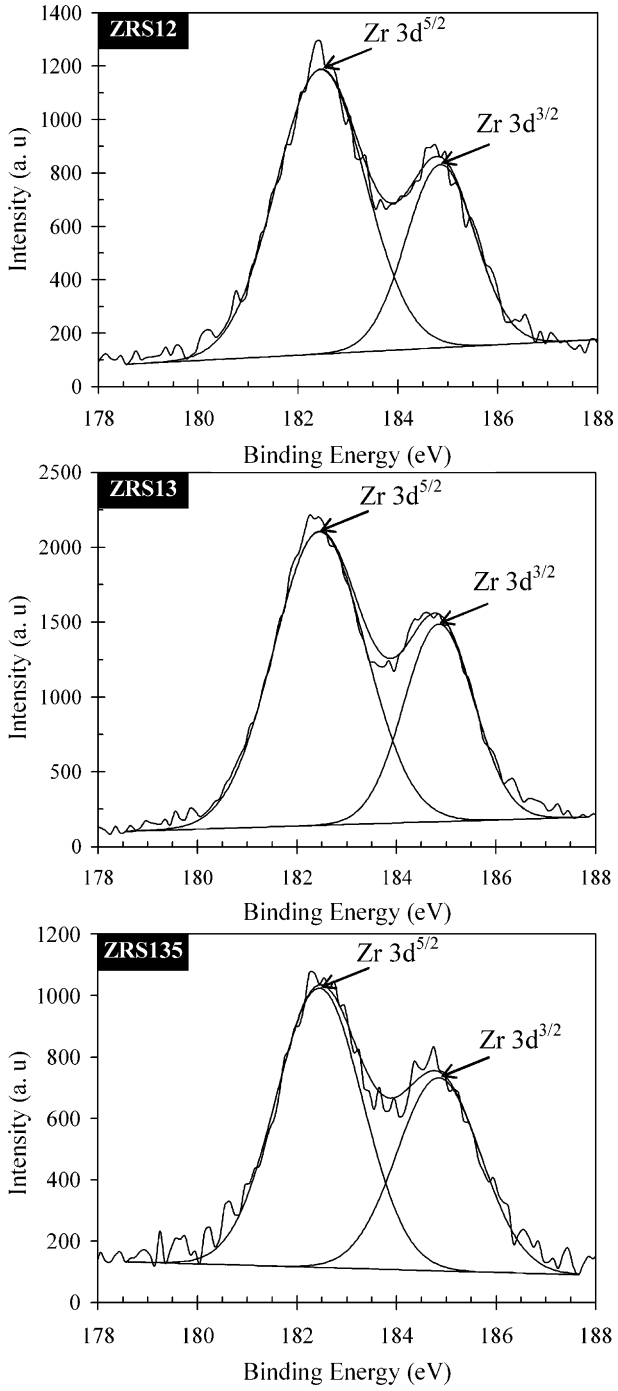

Fig. 10. XPS spectra of Zr 3d electrons.

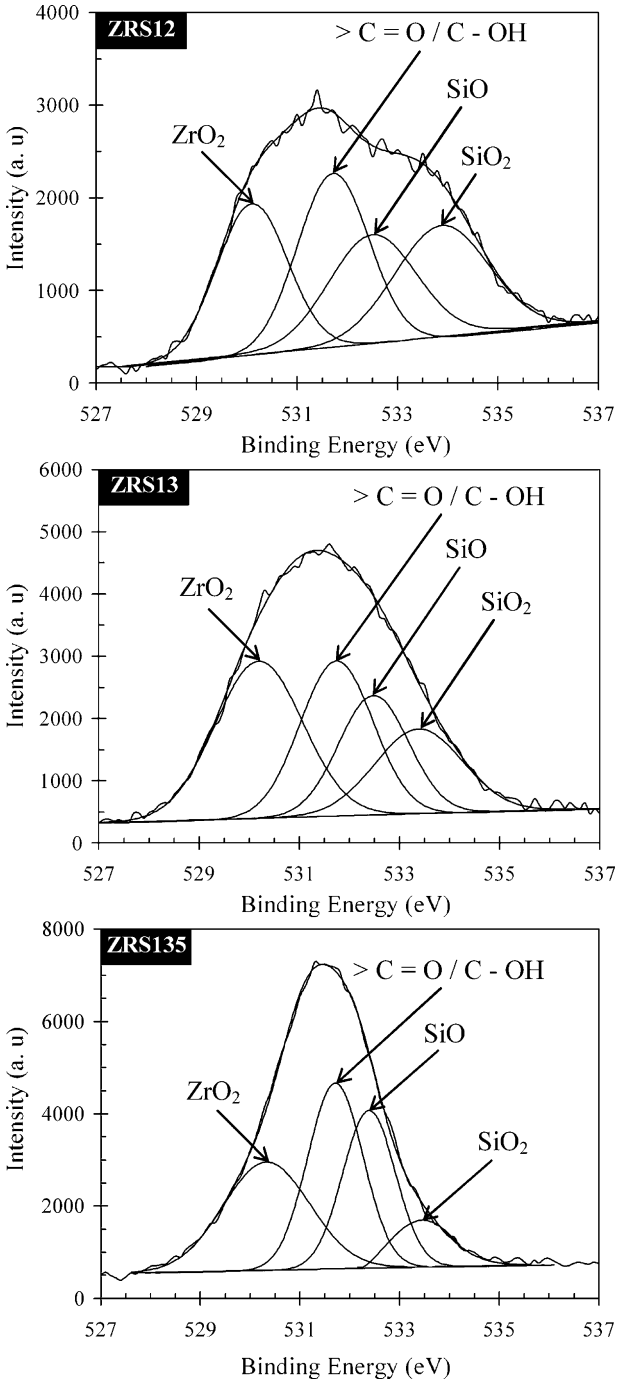

Fig. 11. XPS spectra of O 1s electrons.

Li et al. [25] have prepared silicon carbide by HIPing graphite in a silicon mold at 1700 °C for 2 h under a pressure of 100 MPa. Shi et al. [26] fabricated silicon carbide powders from silicon and phenol resin by heating at 1500 °C in argon atmosphere. This method involved three steps: (1) precursor of powders were produced by coat-mixing process with silicon powders and phenolic resin as a starting materials; (2) precursor powders were converted into carbonized powders by heat treatment at 800 °C in argon atmosphere; (3) the SiC powders were finally synthesized by sintering the carbonized powders at 1500 °C in argon atmosphere. SiC may also be is formed by the reaction of gaseous silicon monoxide (SiO) and carbon monoxide (CO) or carbon (C) in the carbothermal reduction. XPS analyses suggested the reduction of SiO_2 to SiO and then to SiC in the HIPed composites. However, the reaction of SiO and CO becomes thermodynamically favorable when the partial pressure of CO is greater than 0.027 MPa and the temperature is higher than 1300 °C [21]. In addition, in the presence of pores in the composite bodies, carbothermal reactions could occur producing SiO and CO species and when these gaseous species were entrapped in the porous structure, with P_{SiO}/P_{CO} ratio higher than unity, SiC whisker particles

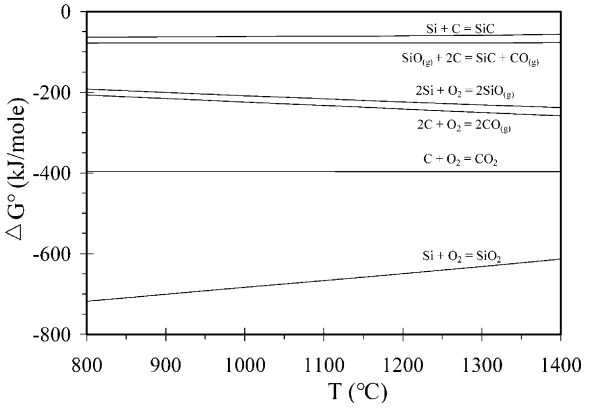

Fig. 12. Change in Gibbs free energy with temperature for the formation of various compounds.

could be produced. The reactions involved in this step can be summarized as [27]

$$SiO_{(g)} + 3CO_{(g)} = SiC_{w(S)} + 2CO_{2(g)} \quad (1)$$

$$2C_{(S)} + 2CO_{2(g)} = 4CO_{(g)} \quad (2)$$

Hence, the overall reaction is:

$$SiO_{(g)} + 2C_{(S)} = SiC_{w(S)} + CO_{(g)} \quad (3)$$

where g = gas, w = whisker and s = solid.

The dissipation of CO gas is required for the above reactions to be maintained. When the open pores in the composites become isolated upon densification, dissipation of CO is impossible and the CO would soon achieve its equilibrium partial pressure in the pores such that the reactions cease [15]. At the same time, further densification will be prohibited because the CO partial pressure in the pores acts against the pressure for pore reduction.

According to XRD, the formation of β-SiC was enhanced with the increase in HIPing temperature. SEM photographs showed that composites exhibit numerous pores with diameters ranging from several μm to several 10 μm and the crystal growth with facets was observed at 1350 °C. The evolution of volatile products (such as CH_4, H_2, CO, CO_2, H_2O, etc.) due to thermal decomposition of phenolic resin caused the formation of pores. In addition, the energy dispersive spectroscopy showed that C/Si atomic ratio was 1:1 in the crystals. This C/Si atomic ratio may be reasonable to be assigned to that of β-SiC, because XRD spectrum obtained from the composite HIPed at 1350 °C also showed the prominent appearance of β-SiC. XPS spectra showed enhancement in the formation of SiC and SiO, and reduction in SiO_2 with the rise in HIPing temperature. The change in Gibbs free energies of CO and SiO are very closely related to each other (Fig. 12). Therefore, according to our experimental results (XRD, EDS, SEM and XPS analyses) and above discussion, we suggest that the nucleation of β-SiC particles might be by the carbothermal reactions of gaseous SiO and CO, as given by Eq. (3). And then these β-SiC particles were grown to several μm in size. In addition, at higher temperatures (1400 °C: below the melting point of Si) the formation of β-SiC particles was enhanced and the formation of β-SiC whiskers was also observed.

5. Conclusions

Three phase mixture of C/SiC/ZrO_2 porous composites with pores size ranging from several μm to several 10 μm were prepared. The nucleation of β-SiC particles might be by the carbothermal reactions of gaseous SiO and CO. In addition, the formation of β-SiC was enhanced at higher temperatures below the melting point of Si and crystal growth of β-SiC with facets was observed at 1350 °C. The hot isostatic pressing led to the increase in density (3.38–3.48 g/cm^3) and reduction in porosity (from 32 to 20%) of the composites. The formation and growth of β-SiC, in addition to the densification of matrices by HIPing, led to the increase in hardness (max.: 13.99 GPa) at higher temperatures. In addition to the fabrication of porous composites, this technique might also be implied to convert the used polymeric materials to produce silicon carbide and to minimize the environmental problems caused by the gases formed during combustion of used polymeric products.

Acknowledgement

We are thankful to Mr. Oozono Yosihisa (from Division of Instrumental Analysis, Frontier Science Research Center, Kagoshima University)) for his assistance in conducting XPS analyses.

References

[1] B.-T. Lee, R.K. Paul, C.-W. Lee, H.-D. Kim, Fabrication and microstructural characterization of continuously porous Si_2N_2O–Si_3N_4 ceramics, Mater. Lett. 61 (11) (2007) 2182–2186.
[2] M.A. Sharif, Y. Nakamura, H. Sueyoshi, Preparation of preform for porous ceramic–matrix-composite by the pyrolysis of phenolic resin, Trans. Mater. Res. Soc. Jpn. 31 (4) (2006) 845–852.
[3] A.K. Gain, J.-K. Han, H.-D. Jang, B.-T. Lee, Fabrication of TiO_2–ZrO_2 coating on continuously porous SiC–Si_3N_4 composites, Surf. Coat. Technol. 201 (3) (2006) 519–525.
[4] T. Isobe, T. Tomita, Y. Kameshima, A. Nakajima, K. Okada, Preparation and properties of porous alumina ceramics with oriented cylindrical pores produced by an extrusion method, J. Eur. Ceram. Soc. 26 (6) (2006) 957–960.
[5] M. Mizutani, H. Takase, N. Adachi, T. Ota, K. Daimon, Y. Hikichi, Porous ceramics prepared by mimicking silicified wood, Sci. Technol. Adv. Mater. 6 (1) (2005) 76–83.
[6] J.-F. Yang, S.-Y. Shan, R. Janssen, G. Schneider, T. Ohji, S. Kanzaki, Synthesis of fibrous β-Si_3N_4 structured porous ceramics using carbothermal nitridation of silica, Acta Mater. 53 (10) (2005) 2981–2990.
[7] Y. Sakka, F. Tang, H. Fudouzi, T. Uchikoshi, Fabrication of porous ceramics with controlled pore size by colloidal processing, Sci. Technol. Adv. Mater. 6 (8) (2005) 915–920.
[8] S. Zhu, S. Ding, H. Xi, Q. Li, R. Wang, Preparation and characterization of SiC/cordierite composite porous ceramics, Ceram. Int. 33 (1) (2007) 115–118.
[9] F.-Z. Zhang, T. Kato, M. Fuji, M. Takahashi, Gelcasting fabrication of porous ceramics using a continuous process, J. Eur. Ceram. Soc. 26 (5) (2006) 67–671.
[10] C. Galassi, Processing of porous ceramics: piezoelectric materials, J. Eur. Ceram. Soc. 26 (14) (2006) 2951–2958.

[11] Y.-J. Lin, C.-M. Chaung, The effects of transition metals on carbothermal synthesis of β-SiC powder, Ceram. Int. 33 (5) (2007) 779–784.
[12] N. Bamba, Y.H. Choa, K. Niihara, Fabrication and mechanical properties of nanosized SiC particulate reinforced yttria stabilized zirconia composite, Nanostruct. Mater. 9 (1–8) (1997) 497–500.
[13] P. Mogilevsky, A. Zangvil, Modeling of oxidation behavior of SiC-reinforced ceramic matrix composites, Mater. Sci. Eng. A 262 (1) (1999) 16–24.
[14] A. Selçuk, C. Leach, R.D. Rawlings, Processing, microstructure and mechanical properties of SiC platelet-reinforced 3Y-TZP composites, J. Eur. Ceram. Soc. 15 (1) (1995) 33–43.
[15] Y.-J. Lin, C.-P. Tsang, Fabrication of mullite/SiC and mullite/zirconia/SiC composites by 'dual' in-situ reaction syntheses, Mater. Sci. Eng. A 344 (1–2) (2003) 168–174.
[16] K.A. Trick, T.E. Saliba, Mechanisms of the pyrolysis of phenolic resin in a carbon/phenolic composite, Carbon 33 (11) (1995) 1509–1515.
[17] G.D. Soraru', S. Modena, P. Bettotti, G. Das, G. Mariotto, L. Pavesi, Si nancrystals obtained through polymer pyrolysis, Appl. Phys. Lett. 83 (4) (2003) 749–751.
[18] H. Geßwein, J.R. Binder, H.-J. Ritzhaupt-Kleissl, J. Haußelt, Fabrication of net shape reaction bonded oxide ceramics, J. Eur. Ceram. Soc. 26 (4–5) (2006) 697–702.
[19] L. Mariappan, T.S. Kannan, A.M. Umarji, In situ syntheses of Al_2O_3–ZrO_2–SiC_w ceramic matrix composites by carbothermal reduction of natural silicates, Mater. Chem. Phys. 75 (1–3) (2002) 284–290.
[20] Z. Liu, W. Shen, W. Bu, H. Chen, Z. Hua, L. Zhang, L. Li, J. Shi, S. Tan, Low-temperature formation of nanocrystalline β-SiC with high surface area and mesoporosity via reaction of mesoporous carbon and silicon powder, Micropor. Mesopor. Matter 82 (1–2) (2005) 137–145.
[21] G.-Q. Jin, X.-Y. Guo, Synthesis and characterization of mesoporous silicon carbide, Micropor. Mesopor. Matter 60 (1–3) (2003) 207–212.
[22] S.-J. Park, Y.-S. Jang, X-ray diffraction and X-ray photoelectron spectroscopy studies of Ni–P deposited onto carbon fiber surfaces: impact properties of a carbon–fiber-reinforced matrix, J. Colloid Interf. Sci. 263 (1) (2003) 170–176.
[23] C.D. Wagner, A.V. Naumkin, A. Kraut-Vass, J.W. Allison, C.J. Powell, J.R. Rumble Jr., NIST X-ray Photoelectron Spectroscopy Database, NIST Standard Reference Database 20, Version 3.4., http://srdata.nist.gov/xps/index.htm.
[24] N. Worasuwannarak, S. Hatori, H. Nakagawa, K. Miura, Effect of oxidation pre-treatment at 220 to 270 °C on the carborization and activation behavior of phenolic resin fiber, Carbon 41 (5) (2003) 933–944.
[25] J.-F. Li, S. Sugimoto, S. Tanaka, M. Esashi, R. Watanabe, Manufacturing silicon carbide by reactive hot isostatic pressing within micromachined silicon molds, J. Am. Ceram. Soc. 85 (1) (2002) 261–263.
[26] L. Shi, H. Zhao, Y. Yan, Z. Li, C. Tang, Synthesis and characterization of submicron slicon carbide powders with silicon and phenolic resin, Powder Technol. 169 (2) (2006) 71–76.
[27] M.A. Schiavon, E. Radovanovic, I.V.P. Yoshida, Microstructural characterisation of monolithic ceramic matrix composites from polysiloxane and SiC powder, Powder Technol. 123 (2–3) (2002) 232–241.